Supplemental methods:

Analysis of lung inflammation. On day 7 or 8, mouse lungs were lavaged with sterile PBS and BALF used for flow cytometric assessment and quantification of immune cells and assessment of total protein and IgM.   In influenza studies, the middle and cranial lobes of the right lung were snap-frozen and homogenized under liquid nitrogen for RNA extraction by an RNA isolation kit (Agilent Technologies). The concentration of total protein in BALF was measured by DC Protein Assay Kit (Bio-Rad) per the manufacturer's protocol. BALF cytokine concentrations were determined by MILLIPLEX multiplex assay using Luminex (EMD Millipore) following the kit protocol and total IgM quantitated by ELISA. Collagen quantification after bleo injury was performed by hydroxyproline assay. Right lungs were removed and cut into small pieces and then digested overnight at 110°C in 20 ml/g of 6 N HCl. After neutralization with 6 N NaCl, the pH was adjusted (6.0 < pH < 10.0). Samples (100 µl) were mixed with 1 ml chloramine T solution (1.4% chloramine T, 10% isopropanol, 0.5 M sodium acetate, pH 6.0) for 20 min at room temperature, followed by incubation in 1 ml Erlich's solution (14.9% p-dimethylaminobenzaldehyde, 70% isopropanol, 20% perchloric acid; Sigma-Aldrich) at 65°C for 15 min. 200 µl of each sample in a 96-well plate was measured for absorbance at 570 nm. The right lung was used consistently to allow appropriate comparisons.

Histopathological evaluations. For histological analyses, lungs were excised and gently inflated with 10% neutral buffered formalin and then fixed for at least 24 hours before trimming, embedding in paraffin, sectioned transversely, and adhered to glass microscope slides. Following automated hematoxylin and eosin staining, whole slide images (WSI) of each slide were captured via a Zeiss Mirax MIDI scanner utilizing a Plan-Apochromat 40x/.95N.A. objective lens, AxioCam MRm digital CCD camera (Carl Zeiss). WSI images were graded for lung pathology by a pathologist blinded to mouse genotype and/or treatment. Perivascular and peribronchial inflammation, intra-alveolar macrophages, and intra-alveolar hemorrhage were semi-quantitatively scored as follows: none: 0; minimal: 1; mild: 2; moderate: 3, and severe: 4. Fibrosis was scored according to Ashcroft et al (1). Percent area of consolidation was determined using digital slide images as follows: total area of lung consolidation/total area of lung sections. Area of consolidation were manually segmented.

Generation of human monocyte-derived dendritic cells (Mono-DC). Peripheral blood mononuclear cells (PBMC) were isolated from fresh normal adult human LeukoPaks (Central Blood Bank) following density gradient centrifugation with Ficoll. CD14$^+$ monocytes were positively selected from PBMC using human CD14$^+$ monocyte isolation kits (Miltenyi Biotec). Mono-DC were generated from CD14$^+$ cells in RPMI containing human AB serum (Corning), IL-4, and GM-CSF as we have described (2). Mono-DC were harvested at day 7 and used to expand isolated human Treg.

*RNA-Seq and bioinformatics analyses.*

RNA-seq libraries were prepared using Ion Total RNA-Seq Kit (Life Technologies) with GeneRead rRNA Reduction kit (Qiagen). Samples were run using an Ion Torrent Proton Sequencer with PI chip and Torrent Suite software v4.2.1 (Life Technologies). The raw Ion Torrent reads were quality trimmed using cutadapt (3). These quality trimmed reads were mapped using 'Two step alignment method for Ion Proton Transcriptome data' as suggested by Life Technologies. The reads were first aligned to GRCm38 mouse Ensembl reference genome using Tophat v2.0.9 (4), then alignment for unmapped reads using bowtie v2.1.0 (5) in local mode. Cufflinks v2.2.1 (6) was used to assemble the transcripts and estimate their abundances. Cuffdiff v2.2.1 (7) was used to perform differential gene expression between the sample sets. A volcano plot using R was generated from the differential gene expression results of Cuffdiff.

qRT-PCR methodology. Total RNA was isolated using TRIzol reagent (ThermoFisher) and Direct-zol RNA miniPrep Plus columns (Zymo Research Corporation). RNA was reverse transcribed using the iScript cDNA synthesis kit (Bio-Rad). *Il10*, *Il13*, *Arg1,* and *18s* messages were amplified with Fast SYBR Green Master Mix (Applied Biosystems) on a StepOnePlus Real-Time PCR System (Applied Biosystems). Data were analyzed using the $2^{-\Delta\Delta CT}$ method (8). Primers for *Il10*, *Il13*, and *Il1rl1* (ST2) were purchased commercially (Qiagen). Primers for *Arginase 1* (*Arg1*) were forward 5′-CAGAAGAATGGAAGAGTCAG-3′and reverse 5'-CAGATATGCAGGGAGTCACC-3'. Primers for *18s* were forward 5′-AACTTTCGATGGTAGTCGCCGT-3′ and reverse 5′-TCCTTGGATGTGGTAGCCGTTT-3′. All qRT-PCR assays were performed in triplicate and data are reflective of no less than three independent experiments.

Supplemental References:

1.   Ashcroft T, Simpson JM, and Timbrell V. Simple method of estimating severity of pulmonary fibrosis on a numerical scale. *J Clin Pathol.* 1988;41(4):467-70.

2.   Macedo C, Turnquist HR, Castillo-Rama M, Zahorchak AF, Shapiro R, Thomson AW, et al. Rapamycin augments human DC IL-12p70 and IL-27 secretion to promote allogeneic Type 1 polarization modulated by NK cells. *Am J Transplant.* 2013;13(9):2322-33.

3.   Martin M. Cutadapt removes adapter sequences from high-througput sequencing reads. *EMBnetjournal.* 2011;17(1):10-2.

4.   Kim D, Pertea G, Trapnell C, Pimentel H, Kelley R, and Salzberg SL. TopHat2: accurate alignment of transcriptomes in the presence of insertions, deletions and gene fusions. *Genome Biol.* 2013;14(4):R36.

5.   Langmead B, and Salzberg SL. Fast gapped-read alignment with Bowtie 2. *Nat Methods.* 2012;9(4):357-9.

6.   Trapnell C, Williams BA, Pertea G, Mortazavi A, Kwan G, van Baren MJ, et al. Transcript assembly and quantification by RNA-Seq reveals unannotated transcripts and isoform switching during cell differentiation. *Nat Biotechnol.* 2010;28(5):511-5.

7.   Trapnell C, Hendrickson DG, Sauvageau M, Goff L, Rinn JL, and Pachter L. Differential analysis of gene regulation at transcript resolution with RNA-seq. *Nat Biotechnol.* 2013;31(1):46-53.

8.   Livak KJ, and Schmittgen TD. Analysis of relative gene expression data using real-time quantitative PCR and the 2(-Delta Delta C(T)) Method. *Methods.* 2001;25(4):402-8.

Supplemental figures and legends
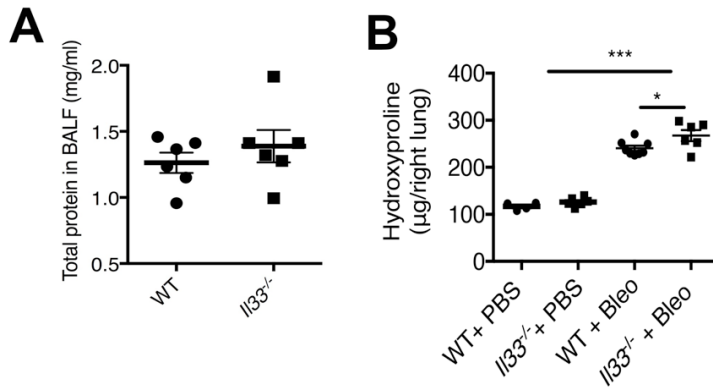
Supplemental Figure 1. (**A**) IL-33 did not significantly affect early levels of total protein in bronchoalveolar lavage fluid (BALF) at days 7-8 post i.t. bleo injection. (**B**) By day 13, however, surviving bleo-treated *Il33*^{−/−} mice displayed significantly increased levels of lung hydroxyproline. Data are mean ± SD P values were determined by two-tailed Student's *t*-test. *$P<0.05$, ***$P<0.001$. Data depicted are from 1 experiment representative of 2 completed and n=4-8 mice per group.
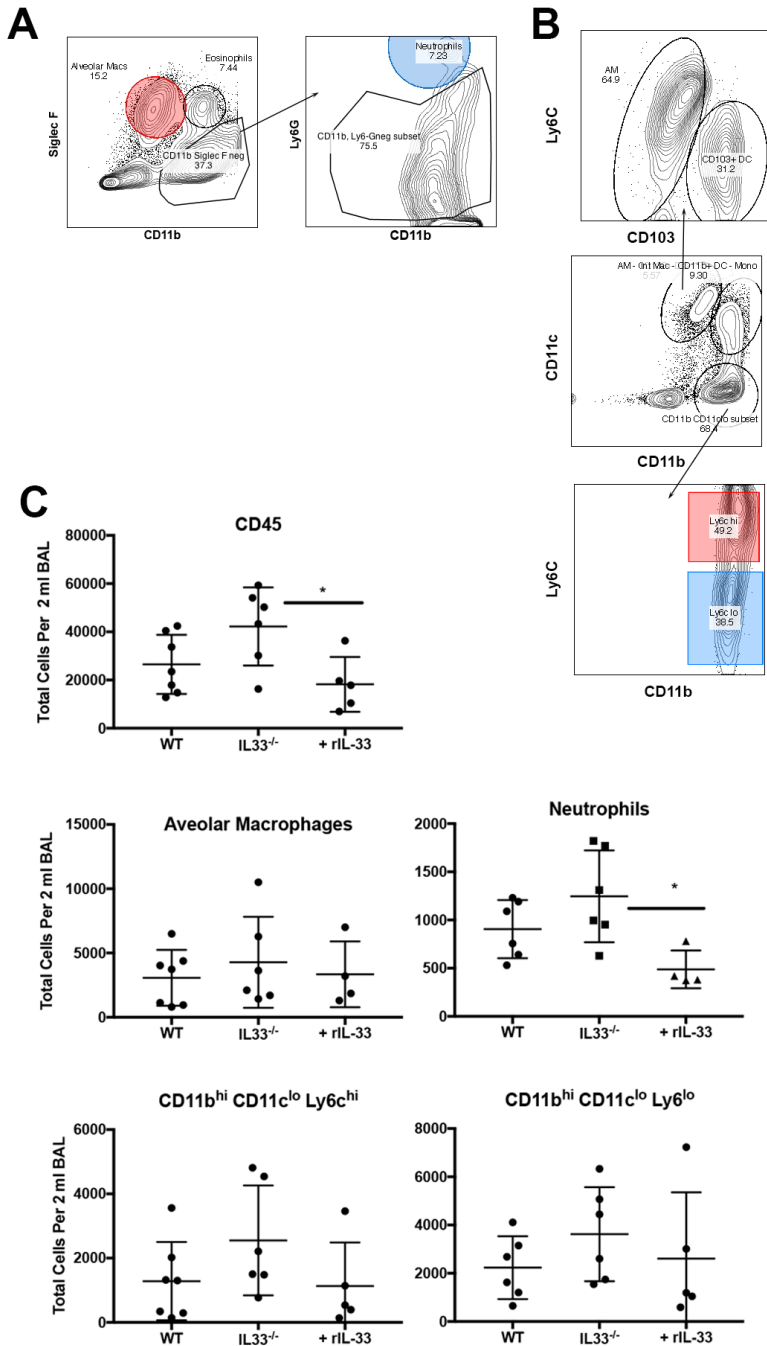
Supplemental Figure 2. (A) Example of gating strategy used for Figure 2 flow cytometric assessment of BALF on day 7 or 8 post i.t. bleo for alveolar macrophages (CD45$^+$ CD11b^{lo} Siglec-F$^+$), eosinophils (CD45$^+$ CD11b^{hi} Siglec-F^{hi}), and neutrophils (CD45$^+$ CD11b^{hi} Siglec-F$^-$ Ly6G^{hi}). (B) Gating strategy used to characterize BALF on day 7 or 8 post bleo for alveolar macrophages (CD45$^+$ CD11b^{lo} Ly6C$^+$ CD103$^-$ Siglec-F$^+$), CD103$^+$ DC (CD11b^{lo} CD103$^+$) and monocytes (CD45$^+$ CD11b^{hi} CD11c^{lo} Ly6C^{hi} or Ly6C^{lo}). (C) Calculated total number of indicated immune population. Data were pooled from 2 independent experiments (n = 5-6 mice per group total) and presented as means ± SD. *P* values were assessed by 1-way ANOVA. *$P<0.05$

A

Lung cells: CD45+ CD3+ CD4+ CD25+

B

C

CD45+ CD11b− CD3+ CD4+

D

E
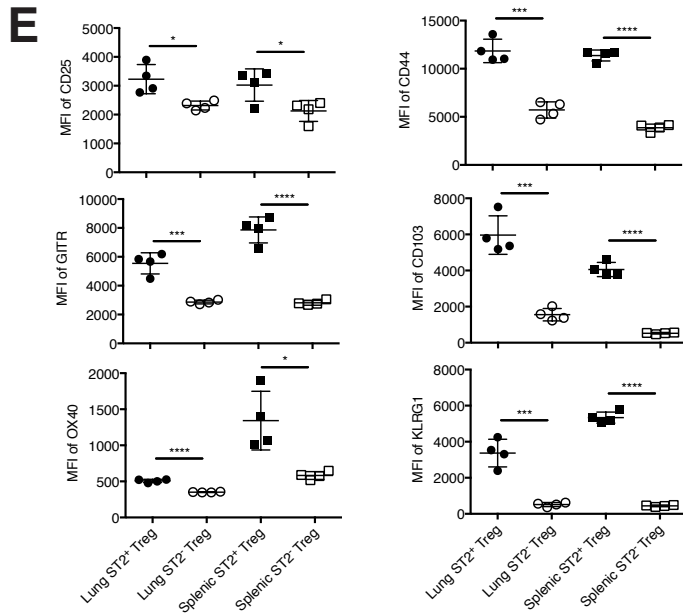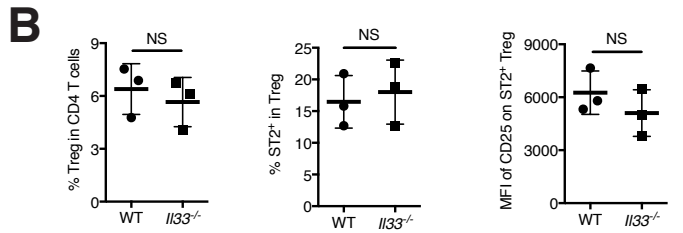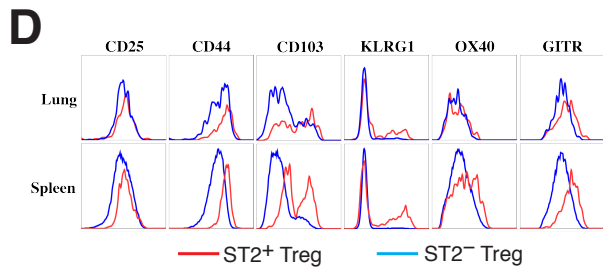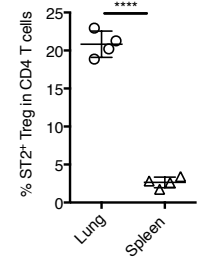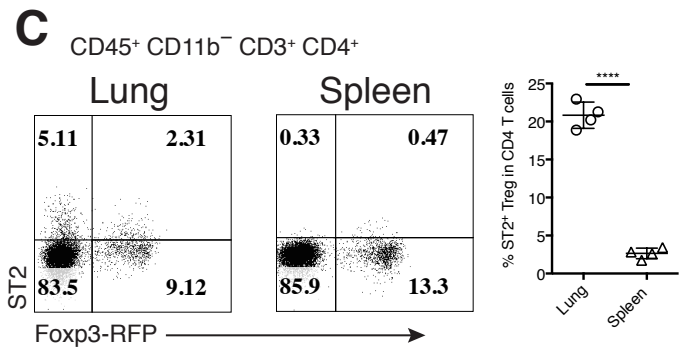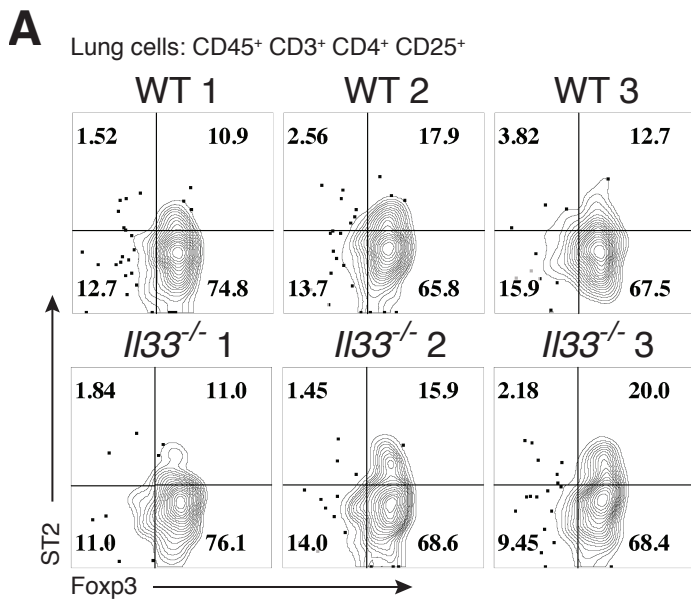
Supplemental Figure 3. A-B. Flow cytometric assessment of CD45+ CD3+ CD4+ CD25+ cells isolated from enzymatically digested naïve WT B6 (n = 3) and B6 *Il33−/−* (n = 3) mouse lungs establishes that IL-33 deficiency does not result in a baseline defect in frequency of lung Treg, including the ST2+ subset. Statistical significance between means ± SD were determined by unpaired, 2-tailed Student's 't' test. (C-E) Flow cytometric comparison of ST2+ and ST2− Treg subsets from the spleen and lung regarding their expression of activation markers including CD44, CD103 and KLRG1, and suppressor functional molecules such as OX40 and GITR. Data are means ± SD *P* values were determined by two-tailed Student's *t*-test. NS, not significant. *P < 0.05, ***P < 0.001, ****P < 0.0001.

A

B
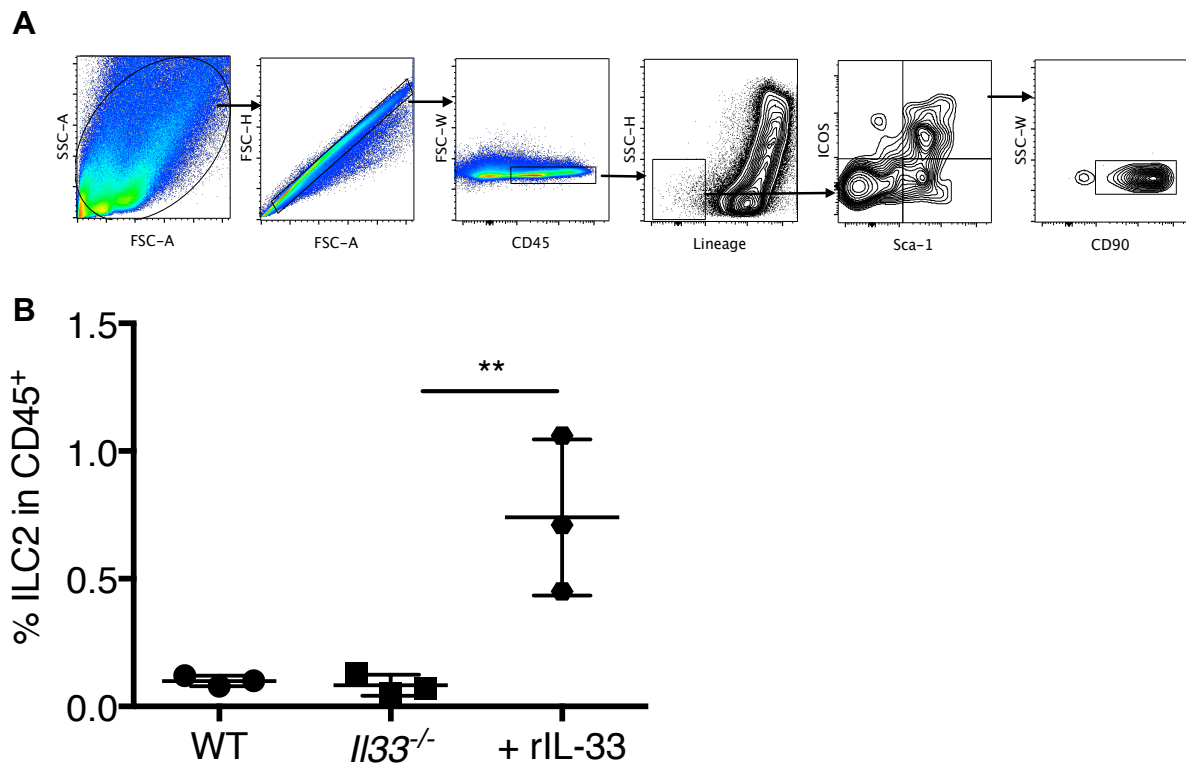
Supplemental Figure 4. The frequency of type 2 innate lymphoid cells (ILC2s; CD45$^+$ Lineage$^-$ ICOS$^+$ Sca-1$^+$) was not reduced in $Il33^{-/-}$ mice after bleo-induced ALI. (**A**) Gating strategy used to assess ILC2 in WT or $Il33^{-/-}$ B6 mice injected i.t. with bleo (1.5 IU/Kg) alone or i.t. bleo and 1 μg recombinant IL-33 (rIL-33). (**B**) Data depicted in B are means ± SD and P value was determined by 1-way ANOVA followed by Turkey multiple comparisons test. ** $P < 0.01$.
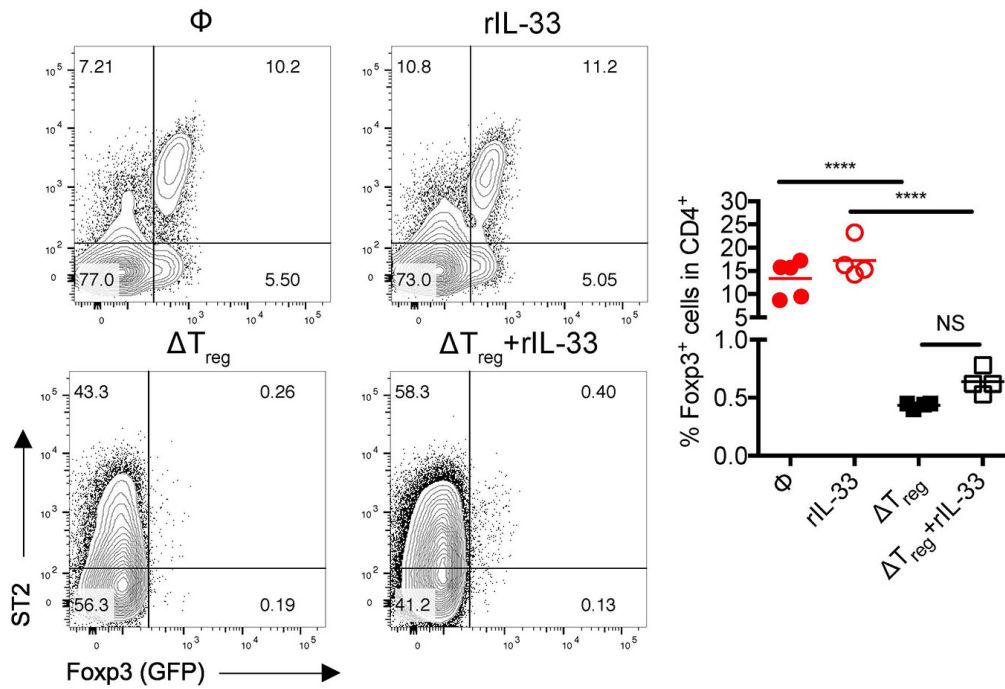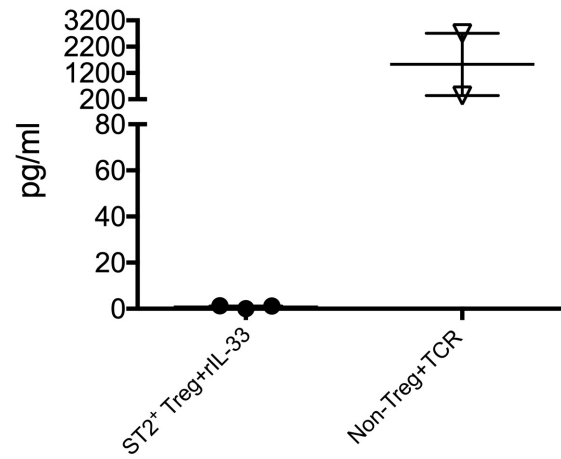
Supplemental Figure 5. Flow cytometric assessment of CD45$^+$CD3$^+$CD4$^+$ cells isolated from enzymatically digested Treg replete B6 *Foxp3^{DTR}* mice lungs at day 8 post bleo (1.0 IU/Kg i.t.) alone (ϕ) or with rIL-33 (1 μg i.t.) compared to those of B6 *Foxp3^{DTR}* mice receiving diphtheria toxin (DT) (15 μg/Kg on day -3, -2 and -1, and every other day i.p. starting from day 1) and bleo and/or rIL-33 treatment at day 0. This analysis establishes that Treg were effectively and comparably depleted by DT during bleo and rIL-33 administration. Depicted data represent 1 experiment with 4-5 mice per group. *P* values were determined 1-way ANOVA. ****$P < 0.0001$.
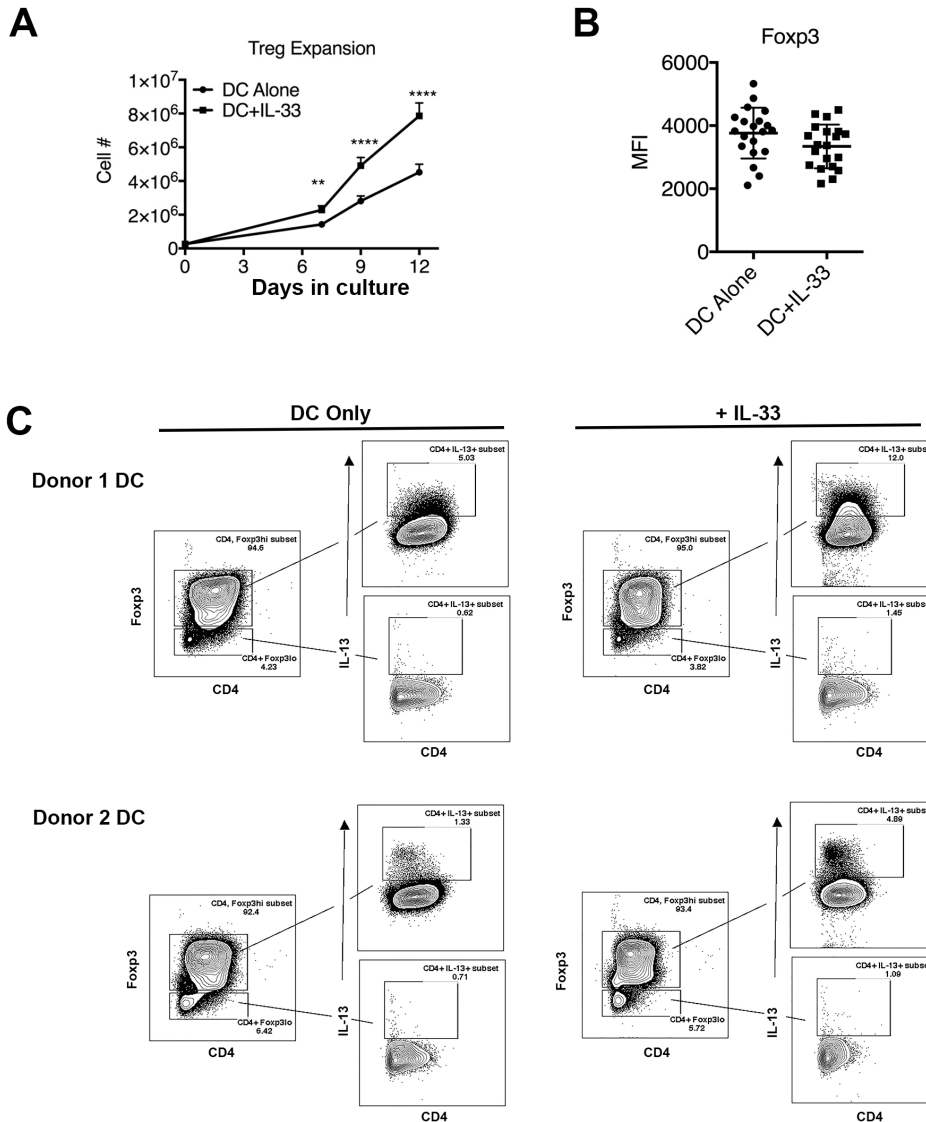
Supplemental Figure 6. Human Treg (CD4^{+} CD25^{hi} CD127^{lo}) were sorted from peripheral blood mononuclear cells and cultured with allogeneic monocyte-derived dendritic cells (Mono-DC) and recombinant human IL-2 (300 U/ml) alone or with recombinant human IL-33 (50 ng/ml) added. **(A)** Absolute count of human Treg cell numbers over the course of culture under the indicated conditions. Data depicted are means ± SD and statistical significance was determined between each condition by unpaired, 2-tailed Student's *t*-test. **$P<0.001$, ****$P<0.0001$. Data represent 8 individual experiments with 18 different Treg and Mono-DC combinations. **(B)** Expression of Foxp3 in total viable cells was quantitated on the 7th day of culture by flow cytometry following intracellular staining. No significant difference between the two groups was observed when the two groups were compared by an unpaired, 2-tailed Student's *t*-test. Lines depict mean ± SD and data are from 8 individual experiments with 20 different Treg and Mono-DC combinations. **(C)** Representative intracellular IL-13 and Foxp3 staining of one Treg sample following 7 days of culture with Mono-DC generated from two different donors and stimulation of cultures with phorbol 12- myristate-13-acetate for 3 h in the presence of golgi plug.
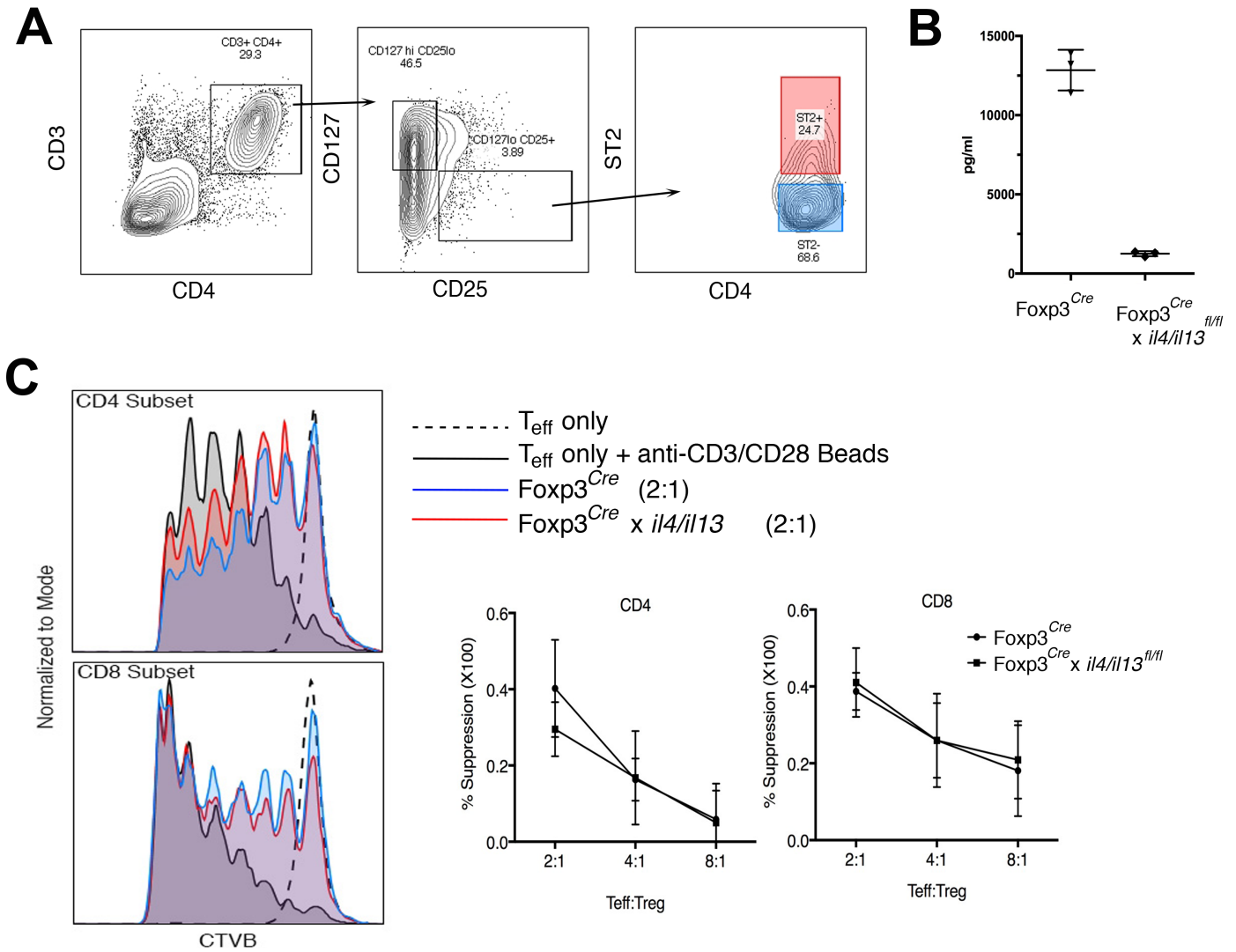
Supplemental Figure 7. (**A**) Depiction of flow sorting design used to obtain ST2$^+$ Treg from BALB/c *Foxp3^{Cre}* and *Foxp3^{Cre}* x *Il4/Il13$^{fl/fl}$* mice for functional assessment. (**B**) CD3$^+$ CD4$^+$ CD25^{hi} CD127^{lo} ST2$^+$ T cells isolated from IL-33-treated *Foxp3^{Cre}* x *Il4/Il13$^{fl/fl}$* mice displayed reduced IL-13 secretion in response to IL-33 (20 ng/ml) compared to those isolated from IL-33-treated *Foxp3^{Cre}* controls. Data are representative of two experiments performed and depict Cytometric Bead Array (CBA) completed for IL-13 on day 3 culture supernatants. (**C**) Sorted CD3$^+$ CD4$^+$CD25^{hi} CD127^{lo} T cells from naïve *Foxp3^{Cre}* and *Foxp3^{Cre}* x *Il4/Il13$^{fl/fl}$* mice displayed similar suppressive capacity. Data are representative of two experiments (n = 6 mice per group).

Supplemental Figure 8. ST2$^+$ CD4$^+$ Foxp3$^+$ (RFP$^+$) were sorted from IL-33-treated Foxp3-IRES-mRFP reporter mice (n=3) and cultured with 20 ng/ml rIL-33 for 3 days. Supernatants were harvested on day 3 of culture and assessed by Cytometric Bead Array (CBA) for IL-4. Sorted CD4$^+$ Foxp3$^-$ (RFP$^-$) T cells stimulated by plate bounds anti-CD3 is provided as positive IL-4 control.

A

B
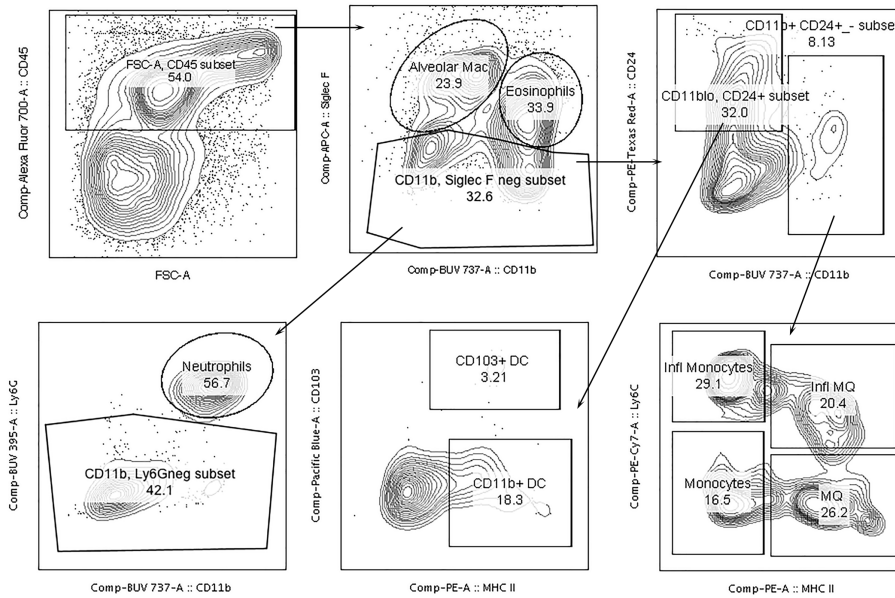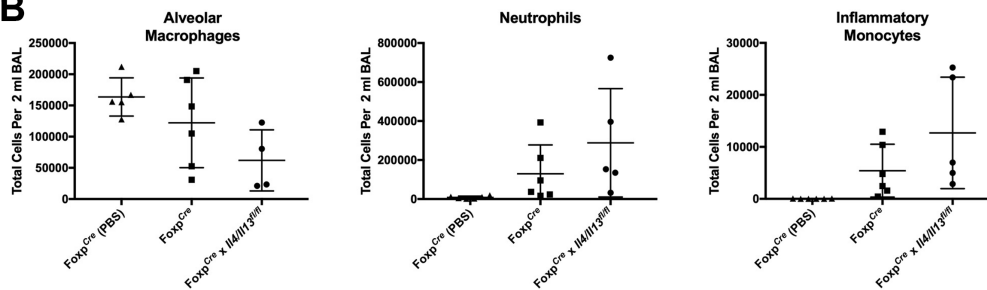
Supplemental Figure 9. **(A)** Gating strategy for Figure 6 flow cytometric assessment of bronchoalveolar lavage fluid (BALF) cells on day 7 post bleomycin (bleo) for alveolar macrophages (CD45$^+$ CD11b^{lo} Siglec-F$^+$), eosinophils (CD45$^+$ CD11b^{hi} Siglec-F^{hi}), neutrophils (CD45$^+$ CD11b^{hi} Siglec-F$^-$ Ly6G^{hi}), CD103$^+$ DC (CD11b^{lo} CD103$^+$ MHC-II$^+$), CD11b$^+$ DC (CD11b^{lo} CD103$^-$ MHC-II$^+$), macrophages (CD45$^+$ CD11b^{hi} CD24l^o MHC-II$^+$ Ly6C^{hi} or Ly6C^{lo}) and monocytes (CD45$^+$ CD11b^{hi} CD24^{lo} MHC-II^{lo} Ly6C^{hi} or Ly6C^{lo}). (B) Calculated total number of indicated immune population. Data were pooled from 2 two independent experiments (n = 5-6 mice per group total) and presented as means ± SD. *P* values were assessed by 1-way ANOVA.
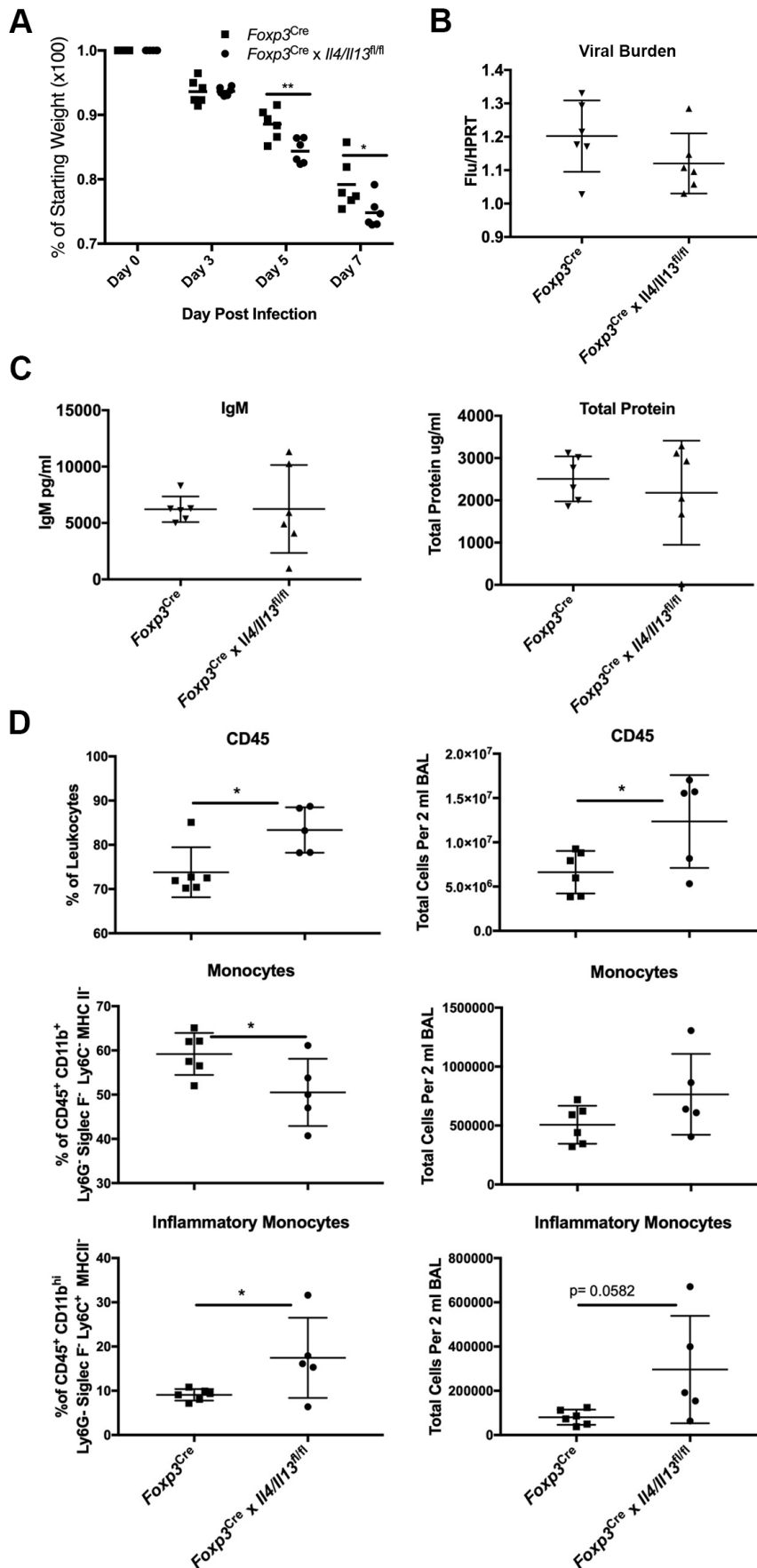
Supplemental Figure 10 (A) Weight loss for BALB/c *Foxp3*[Cre] and *Foxp3*[Cre] x *Il4/Il13*^{fl/fl} mice inoculate with 100 plaque-forming units of influenza. (B) Viral Burden measured by relative expression of influenza mRNA in the right lung on day 7 following influenza inoculation. (C) Total IgM and protein were measured in the BALF on day 7 post-influenza infection (D) Cell counts and frequency assessed by flow cytometric of BALF at day 7 post influenza delivery for leukocytes (CD45^{+}), monocytes (CD45^{+} CD11b^{hi} CD24^{lo} MHCII^{lo}), and inflammatory monocytes (CD45^{+} CD11b^{hi} CD24^{lo} MHCII^{lo} Ly6c^{hi}). (A-D) Data depicted are from 1 experiment (n=5-6 mice per group total). Statistical differences were determined by two-tailed Student's t-test relative to Foxp3[Cre]. *$P<0.05$, **$P<0.01$.